Dyes and Pigments 176 (2020) 108197

Contents lists available at ScienceDirect

Dyes and Pigments

journal homepage: http://www.elsevier.com/locate/dyepig

Photoresponsive N,N′-disubstituted indigo derivatives

Danîela C. Nobre [a], Carla Cunha [a], Alessandro Porciello [b], Federica Valentini [b], Assunta Marrocchi [b], Luigi Vaccaro [b,**], Adelino M. Galvão [c], J. Sérgio Seixas de Melo [a,*]

[a] CQC, Department of Chemistry, University of Coimbra, 3004-535, Coimbra, Portugal
[b] Dipartimento di Chimica, Biologia e Biotecnologie, Università di Perugia, Via Elce di Sotto, 8, 06123, Perugia, Italy
[c] Centro de Química Estrutural, Instituto Superior Técnico (IST), Universidade de Lisboa, Lisboa, Portugal

A R T I C L E I N F O

Keywords:
Indigo
Indigo derivatives
TDDFT
Photochemistry
Ultrafast spectroscopy
Time-resolved fluorescence

A B S T R A C T

The synthesis and a comprehensive characterization of the excited state properties of five N,N′-substituted indigo (**Ind**) derivatives (acetyl-, benzoyl-, methoxybenzoyl-, nitrobenzoyl- and chlorobenzoyl-) was undertaken in various solvents and temperatures. In the excited state, rotation around the central double bond was found with N,N′-diacetylindigo (**DAI**) and N,N′-dibenzoilindigo (**DBI**) derivatives. Both **DAI** and **DBI** acyl derivatives show rotation in the excited state around the central C–C bond, leading to a conical intersection (CI). Steric hindrance prevents **DBI** from accomplishing full rotation (which consequently does not fully isomerize) with two conformers being experimentally found from both fs-transient absorption and time-resolved emission measurements. For **DAI**, the fluorescence decays are single exponential (varying from 2790 ps in 2MeTHF to 7520 ps in MCH), while fs-TA indicates the presence of two species, with lifetimes, in 2MeTHF, of 33 ps and 2790 ps. All the acyl derivatives show blue shifted absorption and emission from the parent indigo dye due to stabilization of the π HOMO orbital in the S_1 π*←π transition by delocalization to the acyl carbonyl. The extent of blue shift among the different acyl derivatives is found to depend on the geometric constraints imposed on the dihedral angle between indigo and the acyl group. With the **DBI** derivatives, interconversion between the two conformers in the excited state leads to rate constant values ranging from 1.3×10^{10} s^{-1} (in MeTHF) to 3.6×10^{9} s^{-1} for the nitrobenzoyl-**DBI** derivative (in dioxane).

1. Introduction

Indigo is one of the most light-stable organic dyes. Associated with its natural origin (it has been extracted from more than 700 Indigofera species) it is a molecule charged of mysticism, with its synthesis linked to the genesis of the modern chemical industry [1–3]. Besides its blue colour, associated to the particular configuration (in H) of N–H and C═O groups connected by a double bond [4], the nature of its high stability has led to a renewed interest in both indigo and also in some synthetic derivatives [5–7]. These include N-alkyl-indigo derivatives [6], imine derivatives [8], ruthenium complexes [9], donor-acceptor copolymers [10], tert-butoxy carbonyl (tBOC) derivatives [11–13] (where reversible *trans-cis* photoisomerizations have been reported) and thioindigo derivatives [14–18]. Indigo's photostability is known to be imparted from an excited state proton transfer (ESPT) involving a single proton transfer from the N–H and C═O groups [2,6]. Photoisomerization (along the central C═C double bond) is a potential competitive pathway for the excited state deactivation, although there are contradictory views, from TDDFT calculations, of this potential deactivation channel in indigo [19,20]. Recent works on related compounds has showed evidence for photoisomerization in both thioindigo and indigo derivatives [13,17,21–23]. *Trans-cis* photoisomerization of indigo derivatives have led recently to the design of indigoid derivatives as potential photoswitches [5].

Trans-cis photoisomerization of N,N′-substituted indigo derivatives has been known since 1968 with the work of Giulliano et al. who reported its existence with N,N′-dimethylindigo and its tetrabrominated derivative, where the *cis* conformer shows an absorption wavelength maximum of 588 nm in benzene [24]. Pouliquen et al. [25] reported the absence of fluorescence for the *cis* form of **DAI** (and other derivatives), while the *trans* form in chloroform showed an emission maximum at 620 nm with a lifetime of 2.1 ns and a fluorescence quantum yield of

* Corresponding author.
** Corresponding author.
E-mail addresses: luigi.vaccaro@unipg.it (L. Vaccaro), sseixas@ci.uc.pt (J.S.S. de Melo).

https://doi.org/10.1016/j.dyepig.2020.108197
Received 8 November 2019; Received in revised form 30 December 2019; Accepted 9 January 2020
Available online 11 January 2020
0143-7208/

0.022. Other groups showed that an increase in solvent viscosity decreases rotation/twisting of the molecule, leading to a decrease in the internal conversion process (i.e. the CI channel becomes less effective), a more efficient triplet state formation and, thus, less efficient *cis* formation [26]. Glowaski et al. [13] have shown that tert-butoxycarbonyl (t-Boc) indigo derivatives present very efficient *trans-cis* photoisomerization; moreover due to their better solubility than indigo and isoindigo, t-Boc derivatives have been used to build-in solution-processed conjugated polymers, with this group readily removed at high temperatures [10,11]. Recently **DAI** *trans-cis* photoisomerization has been studied with fs-TA techniques and shown to be solvent dependent (absent in DMF) [21]. Other N-alkyl and N-aryl indigo derivatives have also been investigated, showing the simultaneous presence of the Z and E isomers in the ground-state [22]. We report a comprehensive characterization of the excited state properties of five N, N′-substituted indigo derivatives as a function of solvent and temperature using fs-Transient absorption (fs-TA), time resolved emission measurements and TDDFT calculations.

2. Experimental section

2.1. Synthesis

Unless otherwise stated, all solvents and reagents were used as obtained from commercial sources without further purification. Dioxane, 2-MeTHF, and dimethyl sulfoxide solvents were all of spectroscopic grade and were purified and dried by conventional methods. Column chromatography was carried out using Silica gel 60, 230–400 mesh. HPLC analyses were performed on an Agilent 1100 instrument equipped with a Phenomenex LUNA® C-18 column (150 mm × 4.6 mm i. d., 3 μm, Torrance, CA, USA), using acetonitrile or THF (HPLC grade) as the mobile phase. ^{1}H and ^{13}C NMR spectra were recorded on a Bruker DRX-ADVANCE 400 MHz operating at 400 MHz, and 100.6 MHz, respectively. IR spectra in the range of 400–4400 cm^{-1} were performed using KBr pellets on a Bruker Tensor 27 FT-IR Spectrometer with a resolution of 4 cm^{-1}. Details of the synthetic procedures for diacetyl- and dibenzoyl indigo derivatives, as well as NMR (^{1}H and ^{13} C) and FT-IR spectra are given as supporting material.

2.2. Material and methods

Absorption spectra were recorded on a Cary 5000 UV–Vis–NIR. Fluorescence spectra were recorded in a Horiba-Jobin-Yvon Spex Fluorolog 3–2.2. spectrophotometer and all spectra were corrected for the instrumental response of the system. The fluorescence quantum yields of the compounds were determined using indigo as standard ($\phi_F = 0.0023$ in DMF) [27]. The molar absorption coefficients (ε_{SS} Table 1) were obtained from the plot of the absorption *vs.* concentration obtained with solutions with concentrations ranging from 8×10^{-5} to 3×10^{-5} mol dm^{-3}. In all cases R^2 values ≥ 0.99 were obtained. For the low temperature measurements (fluorescence quantum yields and emission maxima) these were made with an Horiba-Jobin-Yvon Spex Fluorolog 3–2.2. spectrophotometer and collected in a Dewar with liquid nitrogen. A sample in a quartz EPR-like tube was cooled down with liquid nitrogen (forming a clear glass) and the emission spectra were obtained at this temperature.

Fluorescence decays were measured using a home-built time-correlated single photon counting (TCSPC) apparatus described in detail elsewhere [28]. Briefly, it consists of an PicoQuant Picosecond Laser Diode (with excitation at 451 nm) as excitation source light, a double subtractive Oriel Cornerstone 260 monochromator and an Hamamatsu microchannel plate photomultiplier (R3809U-50). The signal acquisition and data processing is performed with a Becker & Hickl SPC-630 TCSPC module. The fluorescence decays and the instrumental response function (IRF) were collected using 1024 channels in time scales varying from 3.26 to 6.4 ps/channel scale, until 2000–5000 counts at maximum were reached. The full width at half-maximum (fwhm) of the IRF was 0.95–1.10 ns. Deconvolution of the fluorescence decay curves was performed using the modulating function method as implemented by Striker et al. in the SAND program [29] which allows a value of ca. 10% of the fwhm (9 ps) as the time resolution of the equipment with this excitation source.

Femtosecond Transient Absorption Spectroscopy (fs-TA) were performed with a Helios spectrometer (Ultrafast Systems) with an instrumental response function of ~250 fs in an apparatus described elsewhere [6]. The instrumental response function of the system was assumed to be equal to that of the pump−probe cross correlation determined from the measurement of the instantaneous stimulated Raman signal from the pure solvent (in a 2 mm cuvette). To avoid photodegradation, the solutions were stirred during the experiments or

Table 1
Spectral data (including wavelength absorption, λ_{abs} (nm), and emission λ_{em} (nm), maxima, molar extinction coefficient, ε, and Stokes Shift, Δ_{SS}) for Indigo (**Ind**), N,N′-diacetylindigo (**DAI**), N,N′-Dibenzoylindigo in methylcyclohexane (MCH), Dioxane, DMSO and 2-methyltetrahydrofuran (2MeTHF) at room (293K) and low (77K) temperature.

Compound	Solvent	λ_{abs} (nm) 293 K	λ_{em} (nm) 293 K	Δ_{SS} (cm^{-1}) 293K	λ_{abs} (nm) 77 K	λ_{em} (nm) 77 K	Δ_{SS} (cm^{-1}) 77 K	ε (M^{-1} cm^{-1})
Ind	DMSO	619	665	1117				–
	2MeTHF[a]	602	631	763	628	638	250	21424
	Dioxane[a]	601	637	940				22140
DAI	MCH	560	597	1107	549	594	1380	
	DMSO	549	620	2086				5725-
	2MeTHF	561	606	1324				
	Dioxane	550	604	2086				
DBI	MCH	571	600	846	579	620	1142	
	DMSO	577	633	1533				–
	2MeTHF	573	611	1085				6643
	Dioxane	570	612	1204				
DBIOme	DMSO	583	638	1479				–
	2MeTHF	577	615	1071				7459
	Dioxane	577	616	1097				
DBICl	DMSO	573	633	1654				6787-
	2MeTHF	569	610	1181				
	Dioxane	567	612	1297				
DBINO$_2$	DMSO	562	643	2241				3134
	2MeTHF	564	610	1337				
	Dioxane	567	612	1297				

[a] Data from Refs. [27,36].

in movement using a motorized translating sample holder. The spectral chirp of the data was corrected using Surface Xplorer PRO program from Ultrafast Systems [30].

Photoisomerization studies (in the case of DBI) were obtained through irradiation with a high energy laser at 570 nm during 3 min and monitored with an *Ocean Optics* spectrophotometer with absorption spectra collected each 10 s.

All theoretical calculations were of the DFT type, carried out using GAMESS-US version R3 [31]. A range corrected CAMB3LYP [32] functional, with 65% HF exact exchange at long range and 19% at short range, was used in both ground- and excited-state calculations. TDDFT calculations, with similar functionals, were used to probe the excited-state potential energy surface (PES). The LC-BPBE(ω = 0.20 au^{-1}) functional as implemented in GAMESS-US [31] was used to compute unscaled excitation energies in all the stationary points. The solvent was included using the polarizable continuum model with the solvation model density to add corrections for cavitation, dispersion, and solvent structure. In TDDFT calculation of FC (Franck-Condon) excitations the dielectric constant of the solvent was split into a "bulk" component and a fast component, which is essentially the square of the refractive index. In "adiabatic" conditions only the static dielectric constant is used. A 6-31G** basis set was used in either DFT or TDDFT calculations. CAMB3LYP slightly overestimates excitations with a scaling correction applied to the reported values ($E_{reported} = E_{TDDFT} \times 0.92–0.1$) [33]. Excitations were corrected for Zero Point Vibrational Energy by using, essentially, the frequency of the relaxing vibrational mode ($\pm$0.05 eV). The results obtained with the LC-BPBE(20) functional are unscaled raw data from calculations.

3. Results and discussion

3.1. Absorption and fluorescence spectra

Scheme 1 shows the structures and acronyms of the five compounds studied.

Fig. 1 depicts the absorption and fluorescence emission spectra of the five compounds investigated (with indigo, **Ind**, included for comparison) in 2MeTHF and DMSO at room temperature (293 K). Fig. 2 presents the absorption and fluorescence spectra of **DAI** and **DBI** in methylcyclohexane at room (T = 293 K) and low (T = 77 K) temperatures. Spectral and photophysical data are given in Tables 1 and 3 to 5, respectively.

From Figs. 1 and 2 and Table 1 it can be seen that, with the exception of indigo where the H-chromophore [34] seems to play a dominant role, the acetyl substitution leads to the shortest absorption (and emission) wavelength maxima, see Table 1. It is interesting to note that the Stokes Shifts follow the order **DAI** > **DBI** > **IND**. Analysis of Table 1 also suggests that the smaller value of the Stokes shift (Δ_{SS}) for **Ind** is due to the similarity between the ground state and the S_1 geometries [1,6,35,36]. The larger SS in **DAI** and **DBI** indicates the existence of differences in the potential energy curves, which are associated with different structures in the ground-state (GS) and excited state (ES) of these two compounds. However, the most interesting feature is the large Stokes shift (Δ_{SS}) with the two compounds, in particular when compared with **Ind**, see Table 1. With **Ind** the small Δ_{SS} indicates that in the ground state the hydrogen bonds connecting the N–H and C═O groups keep the molecule in a stable *trans* form and that both the excited state keto and enol forms are structurally similar to the GS structure. In contrast, with **DAI** and **DBI** there is a marked difference between the GS and ES geometries.

From Table 1 it can also be seen that the Stokes Shift (SS) is smaller in 2MeTHF than in the other two solvents for both **DAI** and **DBI**. Introduction of the methoxy (**DBIOme**), chloro (**DBICl**), and nitro (**DBINO$_2$**) substituents in the benzoyl group of **DBI**, leads to changes in the absorption and emission wavelength maxima and Δ_{SS}. The Δ_{SS} in DMSO for the **DBINO$_2$** derivative in comparison with **DBI** (2241 cm^{-1} vs. 1533 cm^{-1}) is particularly worthy of note. **DAI** has the highest Stokes shift, which indicates the biggest difference between the S_0 and S_1 geometries. This was further supported by TDDFT calculations (see below).

Previous studies have shown that in solvents of low polarity, such as isooctane, CCl_4, $CHCl_3$ and benzene, the wavelength maxima is, for N, N′-dimethylindigo, found at ~559–560 nm [37]. The ***cis*** form of **DAI** in CCl_4 has been associated with a broad band spanning from 360 to 570

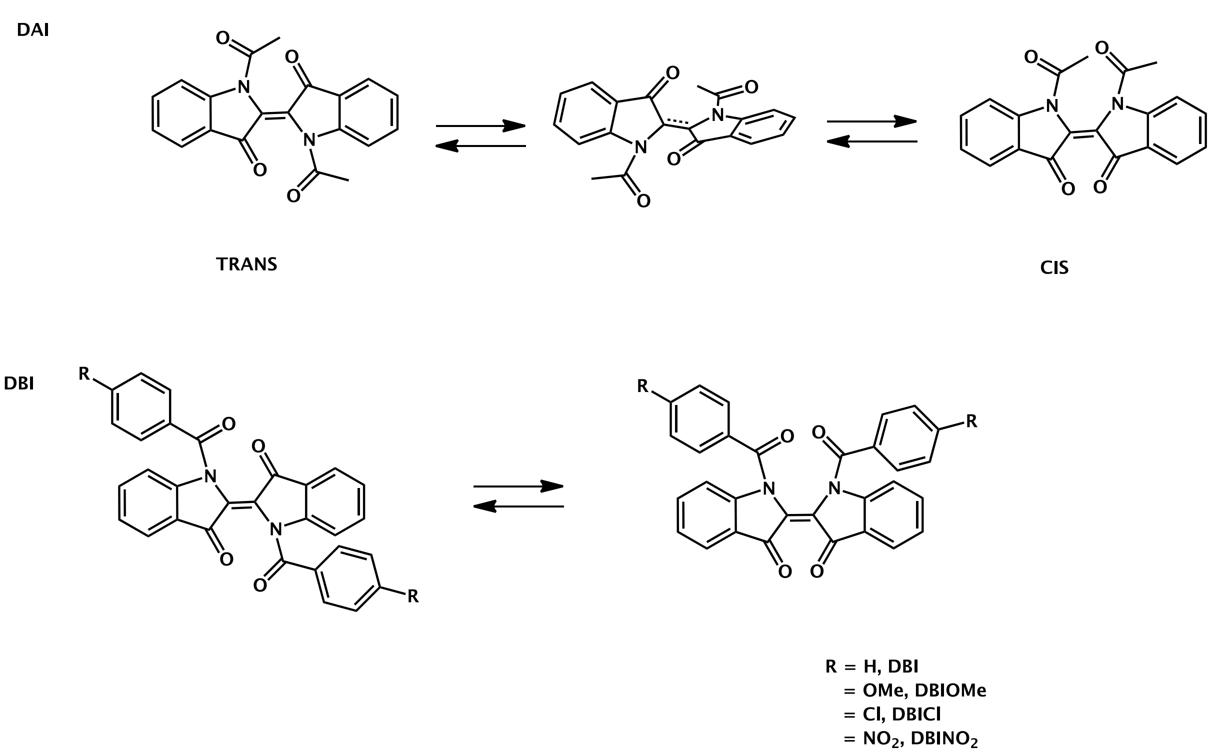

Scheme 1. Structures and acronyms of the DAI and DBI derivatives investigated. The *trans-to-cis* photoisomerization scheme is also shown.

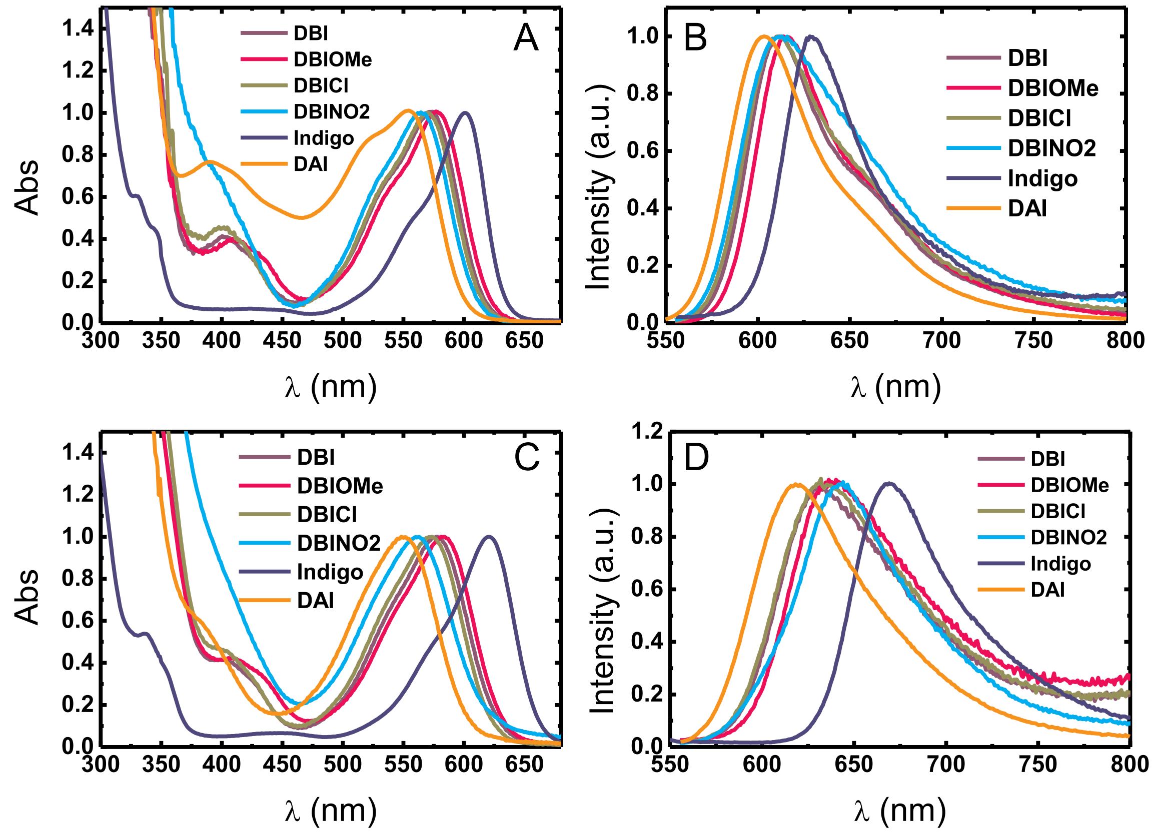

Fig. 1. Absorption (A, C) and fluorescence emission (B, D) spectra of Indigo (**Ind**), N,N′-diacetylindigo (**DAI**), N,N′-dibenzoylindigo (**DBI**) and N,N′-dibenzoylindigo derivatives (**DBIOMe**, **DBICl**, **DBINO2**) in 2MeTHF (top hand panels A and B) and DMSO (bottom hand panels C and D) at T = 293K, with concentrations in a range between 1.5×10^{-6} M – 2.3×10^{-6} M for all compounds and $\lambda_{exc} = 520$ nm.

nm with maximum at ~ 440 nm [38]. Other groups have also reported the formation of *cis* derivatives of indigo diimines, although in these derivatives this form displays maxima at longer emission wavelengths (>650 nm) than the ***trans*** isomer [8].

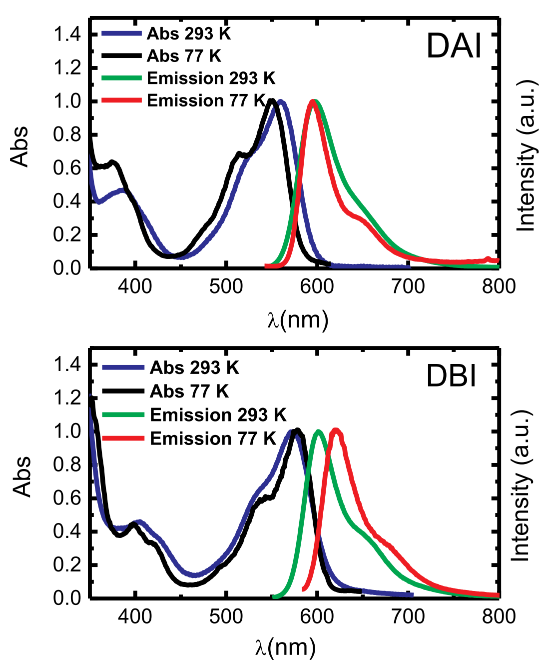

Fig. 2. Normalized absorption and emission spectra for **DAI** (top) and **DBI** (bottom) in methylcyclohexane at T = 293K and 77 K. The absorption spectra at T = 77 K are given by the fluorescence excitation spectra.

3.2. TDDFT calculations

The difference between the emission spectra and maxima of **DAI** and **DBI** in Fig. 2 and Table 1 are worth noting. With the former, the fact that emission spectra and maxima at 293 and 77K are very similar indicates the possibility of free rotation leading to a single (and more stable) conformer in the excited state. In the case of **DBI,** the 20 nm shift of the emission maxima at 77K relative to 293 K indicates that the most stable form (conformer A in Fig. 3 and Table 2) is likely to be the only species present at low temperature, while at 293 K, two conformers are detectable (see Fig. 3 and Table 4).

This experimental data is supported by TDDFT calculations. Although it seems clear that there is a change in the nature of the excited state in N,N′-substituted indigo derivatives, the structural explanation for this is still under discussion, and clearly depends on the substitution. One of the difficulties in the analysis of DFT data for this family of indigo derivatives is the existence of various conformers corresponding to different orientations of the acyl group. DFT calculations on the three conformations where convergence to a local minimum was achieved show that **DAI** has one conformer that is 10 and 24 kJ/mol more stable than the two others; consequently, a single conformer is observed experimentally (with a maximum 2% contribution from the **A** conformer that can be marginally detected in **fs-TA** spectra but not from the time-resolved fluorescence measurements, *see below*). In contrast, with **DBI** the conformers are separated by just 4 and 6 kJ/mol, which allows the experimental detection of two conformers. This is illustrated in Fig. 3, where with **DAI** a single conformer is predicted (Fig. 3 **B** top and Table 2), while with **DBI** an ensemble of three conformers (Fig. 3 bottom) should be considered.

This is further complemented by the fluorescence decays collected along the emission band, which are bi-exponential, with two identical decay times but different pre-exponential factors, and is supported by fs-

Table 2
TDDFT data (LC-BPBE/Scaled[d] CAMB3LYP) including the wavelength maxima for the different conformers A and B for DAI and A, B and C for DBI together with the S_0->S_n predicted transitions and the relative stability and abundance of the conformers at T = 293 K together with the experimental maxima for $S_1 \leftarrow S_0$ transition for **DAI** and **DBI** in DMSO.

Compound	λ_{abs} (nm) $S_1 \leftarrow S_0$	*f*	λ_{abs} (nm) $S_n \leftarrow S_0$	*f*	λ_{em} (nm)	*f*	Relative stability (kJ/mol)	Relative abundance (% at 293K)	λ_{abs} (nm) $S_1 \leftarrow S_0$ Exp.[b)]
DAI (B)	549/551	0.11/0.16	387/390 ($S_{n=3}$)	0.12/0.10	636/616	0.12/0.18	0	98	550
DAI (A)	550/551	0.11/0.16	388/397 ($S_{n=3}$)	0.11/0.10	a)		10	2	
cis-DAI	528/506	0.02/0.06	423/430 ($S_{n=2}$)	0.17/0.16	*forbidden*		34		520[c)]
DBI (A)	564/567	0.11/0.16	398/405 ($S_{n=3}$)	0.07/0.09	662/643	0.13/0.19	0	80	570
DBI (B)	556/559	0.11/0.15	394/400 ($S_{n=3}$)	0.11/0.10	628/612	0.13/0.18	4	15	
DBI (C)	558/561	0.13/0.18	411/412 ($S_{n=3}$)	0.11/0.09	a)		6	5	
cis-DBI	537/522	0.03/0.09	436/445 ($S_{n=2}$)	0.25/0.22	*forbidden*		26		

a S_1 PES was not probed for isomers that differ by more than 5 kJ/mol from the most stable parent structure.
b Experimental data from Table 1 in dioxane.
c From Fig. 6.
d See experimental section for details on the scaling correction.

Table 3
Photophysical data for Indigo (**IND**), **DAI**, **DBI** and **DBI** derivatives in various solvents at room (293K) and low (77K) temperature.

Compound	Solvent	ϕ_F 77 K	ϕ_F 293K	τ_F (ns) 293 K	k_F (ns^{-1}) 293 K	k_{NR} (ns^{-1}) 293 K
IND[a)]	DMSO	–	0.0019	0.117	0.0162	8.5308
	2MeTHF	0.041	0.0019	0.128	0.0148	7.7977
DAI	MCH	0.11	0.06	7.5	0.0080	0.1253
	DMSO	–	0.0058			
	2MeTHF	–	0.028	2.79	0.0100	0.3484
DBI	MCH	0.1	0.011	13.2	0.0008	0.0749
	DMSO	–	0.0012			
	2MeTHF	–	0.0071	4.9	0.0014	0.2026
DBIOMe	DMSO	–	0.001	ND		
	2MeTHF	–	0.0069	6.06	0.0011	0.1639
DBICl	DMSO	–	0.001	0.110[b)]	0.009	9.0818
	2MeTHF	–	0.0057	4.01	0.0014	0.2480
DBINO$_2$	DMSO	–	0.001	0.160[b)]	0.00625	6.2438
	2MeTHF	–	0.0045	2.39	0.0019	0.4165

a) For indigo data is from Ref. [6].
b) Major component of a bi-exponential decay.

Table 4
Fluorescence decay times (τ_i) and preexponential factors (a_i) for **DAI**, **DBI** obtained in 2MeTHF and dioxane at T = 298 K from ps time resolved fluorescence measurements.[a)].

Compound	λ_{em}	Solvent	τ_1 (ps)	a_1	τ_2 (ps)	a_2	k_{INT} (s^{-1})
DAI	598	MCH	-	-	7520	1	NA
DAI	606	2MeTHF	–	–	2790	1	NA
DBI	605	MCH	100	0.820	13200	0.180	1.0E+10
DBI	690	Dioxane	90	0.939	4780	0.061	1.1E+10
DBI	620	2MeTHF	80	0.878	4980	0.122	1.3E+10
DBI	690	2MeTHF	80	0.941	4980	0.059	1.3E+10
DBI Ome	610	Dioxane	110	0.842	5580	0.158	9.1E+09
DBI Ome	690	Dioxane	110	0.953	5580	0.047	9.1E+09
DBI Ome	620	2MeTHF	90	0.902	6060	0.098	1.1E+10
DBI Ome	690	2MeTHF	90	0.957	6060	0.043	1.1E+10
DBI Cl	690	DMSO	110	0.938	430	0.061	9.1E+09
DBI Cl	610	Dioxane	160	0.805	4150	0.195	6.3E+09
DBI Cl	690	Dioxane	160	0.924	4150	0.076	6.3E+09
DBI Cl	610	2MeTHF	140	0.868	4010	0.132	7.1E+09
DBI Cl	670	2MeTHF	140	0.944	4010	0.056	7.1E+09
DBI NO$_2$	670	Dioxane	280	0.932	3030	0.068	3.6E+09
DBI NO$_2$	610	2MeTHF	230	0.85	2390	0.147	4.3E+09

NA = not applicable.
a) Fluorescence decays and analysis can be found in Fig. SI 10–21.

TA data (see discussion below). It is worth noting that a value of 21.77 kJ/mol in hexadecane has been reported in the literature for rotational isomerization around the single bond involving the anthryl and ethenic groups of the S_1 state of 2-vinylanthracene. Here, the presence of two rotamers was confirmed by the bi-exponential nature of the fluorescence decays (*see discussion below*) [39,40].

Table 2 summarizes the TDDFT calculations on the absorption and emission wavelength maxima for the ***trans*** and ***cis*** conformers and different conformers of **DAI** and **DBI**. With both the LC-BPBE (data directly obtained from the calculations and CAMB3LYP (where a scaling factor is added, see experimental section and refs. [6,17,33]), the obtained values are very close (in nm) to the experimental values. It is worth noting that a second allowed band in these derivatives corresponds to a transition to S_3. Observing Figs. 1 and 2 and Table 2 the shoulders in the main absorption bands (~500–530 nm and ~400–430 nm) are likely to be due to the pre-existence of a small quantity of the *cis*-isomer. This effect is more pronounced in non-polar solvents.

The $\pi^* \leftarrow \pi$ nature of the lowest energy absorption band can be seen in Fig. 4, where a sizable delocalization to the acyl carbonyl is only observed with the HOMO. The lowering of the HOMO energy is responsible for the blue shift observed in all the acyl derivatives (Table 1).

The $\pi^* \leftarrow \pi$ excitation transforms the central C=C double bond into a single one, allowing the relative rotation of the two isatin-like moieties. This leads to a peaked Conical Intersection (CI), which provides a competitive deactivation path to fluorescence. The *cis* or *trans* ground state isomers produced will depend on the momentum and point of deactivation in the CI branching coordinate. At the CI the two isatin-like half moieties are found nearly perpendicular to each other and the C=O group nearly planar with the indole moiety, Fig. 5. The structures were optimized in the S_1 PES following a rotational negative eigenvalue of the Hessian, until the gap S_0/S_1 became zero (or very close to zero; in any case always bellow a threshold value of 0.01 eV).

Table 5
Time Resolved fs-TA data (decay times, τ_i, and pre-exponential factors a_i) for **DAI, DBI** and **DBI derivatives** in 2MeTHF and DMSO obtained with λ_{exc} = 530 nm at λ = 611 nm (for **DBI** and **derivatives**) and λ = 598 nm (for **DAI**) in the ESA band. (TA Bands and Time resolved Experiments can be found at SI – Fig. SI4 to 9).

Compound	Solvent	τ_1 (ps)	a_1	τ_2 (ps)	a_2
DAI	2MeTHF	33	0.18	2790	0.82
DBI	2MeTHF	53	0.89	4980	0.11
DBI	DMSO	24.5	0.6	115	0.4
DBI Ome	2MeTHF	65	0.93	4590	0.07
DBI Ome	DMSO	66.4	0.95	1720	0.05
DBI Cl	2MeTHF	94	0.89	3070	0.11
DBI Cl	DMSO	98.5	0.93	642	0.07

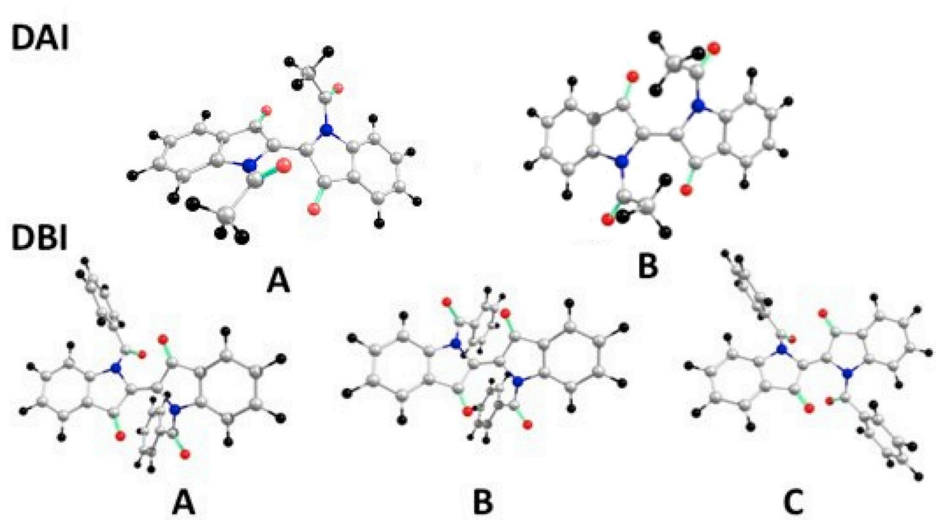

Fig. 3. Geometries for the most stable structures for **DAI** (top) and **DBI** (bottom) obtained from TDDFT calculations.

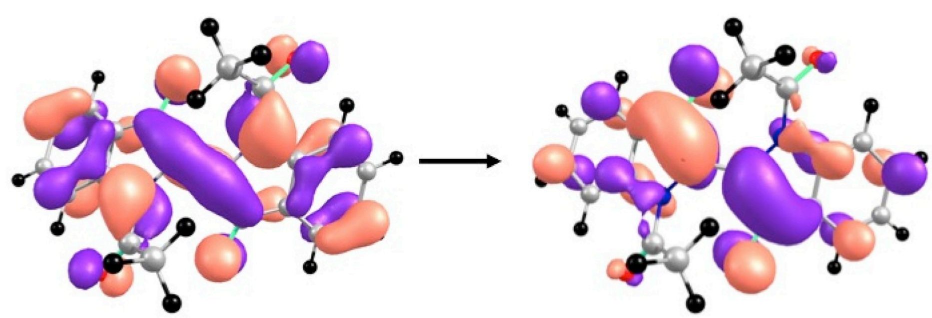

Fig. 4. π→π* transition in **DAI**. Only the HOMO is significantly delocalized onto the acyl group.

3.3. Photochemical studies

For indigo, due to the ground-state hydrogen bonds between the N–H and the C═O groups, the molecule is in a stable and planar form precluding rotation (and isomerization) around the central carbon-carbon bond [2,6,41]. With **DAI** and **DBI,** this is no longer a limitation and photoisomerization is possible. Indeed, the formation of *cis* was confirmed in **DAI** in the present study upon irradiation with a 150 W Xe lamp but found absent in **DBI** (see Fig. 6) in these conditions.

For **DBI** the spectra resulting from the photoisomeration process were obtained with a high energy fs-TA sapphire-titanium laser (see experimental section). The data is presented in Figs. SI1-3 for **DBI**, **DBIOMe** and **DBICl** respectively. In the case of **DBINO$_2$** no spectra could be obtained due to sample degradation.

Moreover, from Fig. SI1 it can be seen that in the non-polar solvent 2MeTHF *trans-cis* isomerization is present and therefore the *cis* form is observed. However, in polar solvents such as DMSO there is no evidence for photoisomerization both for **DAI** and **DBI** due to an over stabilization of the *trans* form relative to the *cis* form [17].

This high requirement in energy for isomerization with **DBI** can be understood by the much higher steric hindrance of this compound reflected in the structural parameters (DFT) N–C═C–N and C–N–C-R (R = Me or Ph) dihedral angles of respectively 5.2° and 13.4° for **DAI** and 9.3° and 20.0° for **DBI**, Fig. 7. Dynamic factors, namely the viscosity of the solvent, may also play a role in precluding the isomerization of **DBI** which indeed involves extra rotations of the phenyl group, which are not

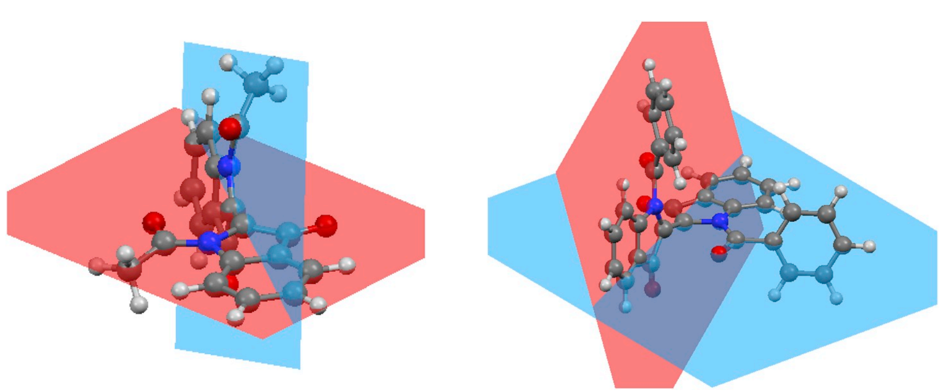

Fig. 5. Structure of **DAI** at the CI (Conical Intersection) (left). A similar structure is found for **DBI** (right).

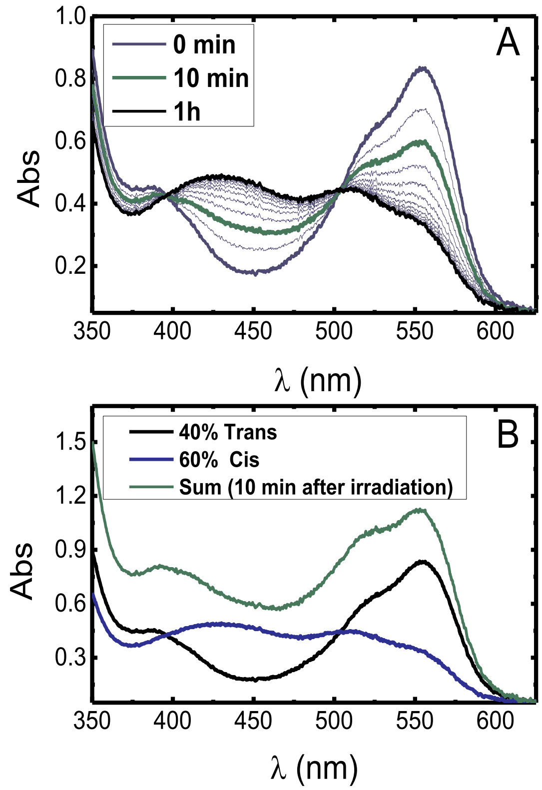

Fig. 6. (**A**) Variation of the absorption spectra of **DAI** in benzene (with the addition of 2 drops of glacial acetic acid) with time, obtained with irradiation at $\lambda_{exc} = 550$ nm (with a Xe lamp of 150W). (**B**) Spectral decomposition of the **DAI** spectra in the Trans (40%) and Cis (70%) forms together with the spectra resulting from sum of both contributions (the 10 min after irradiation plot). For DBI and derivatives (OMe and Cl) see Fig. SI 1–3.

relevant with the methyl derivative (**DAI**).

3.4. Photophysical studies

Photophysical data, including fluorescence quantum yields (φ_F) at T = 293 K and T = 77 K, lifetimes and rate constants for the radiative (k_F) and radiationless (k_{NR}) processes, at T = 293K, are given in Table 3. For indigo the τ_F value is associated to the longest component in the decays, i.e., the enol species formed upon excitation and decay of the keto form [19,35,36]. The φ_F values for **DAI** and **DBI** derivatives were found to be always lower in polar solvents when compared to non-polar ones (up to one order of magnitude), which is further mirrored by the short fluorescence lifetime values. In the polar solvent DMSO, **DAI** and **DBI** have the lowest fluorescence quantum yields ($\sim 10^{-3}$) and lifetimes (in the ps time range), whereas in non-polar solvents (MCH and 2MeTHF) the φ_F values are one order of magnitude higher and the τ_F values are now also higher and within the ns time range (Table 3). This has implications in the radiationless rate constant values, which are 2–3 orders of magnitude higher than the radiative rate constant values in polar solvents. This effect has previously been reported with thioindigo derivatives, and explained by a more accessible CI (in polar solvents) and an increased stabilization of the trans form [17]. The fluorescence quantum yields at 77K increase by approximately one order of magnitude relative to those at RT. This suggests that rotation around the central C–C bond is now blocked both for **DAI** and **DBI** making the access to the CI less effective, such that fluorescence is now a much more effective deactivation channel.

3.5. Time resolved fluorescence and fs-TA transient data

A more detailed analysis of the time resolved fluorescence decays and fs-TA spectra and decays was performed with **DAI** and all the **DBI** derivatives, which can be seen in Tables 1 and 2 and in SI (Fig. SI4 to SI9 for fs-TA data and Fig. SI10 to SI21 for the fluorescence decays).

As was found with related systems, such as 2-VA [40], the time dependent intensity profiles collected along the emission band of **DAI** and **DBI** derivatives are given by a sum of discrete exponentials:

$$I_{A*}(t) = \sum_i a_i e^{-\lambda_i t} \tag{1}$$

where A* is the excited indigo derivative (**DAI** or **DBI**), λ_i is the reciprocal of the decay times, τ_i, and a_i the associated pre-exponential factors.

Table 4 shows that a single exponential properly fits the decays for **DAI**, with values of a few ns (from ~2.8 ns to 7.95 ns). This contrasts with indigo, where the decay times associated with the keto and enol forms are in the range 5–20 ps (keto) and 120–150 ps (enol). However, with **DBI** and its derivatives, the behavior is different, and bi-exponential fluorescence decays are observed, which shows two components/species are present in the excited state. Since the excitation spectra match the absorption spectra, this suggests that the two components are the result of an excited state process, which is due to the presence of at least two conformers separated by ≤ 5 kJ/mol, probably the species A and B in Table 2. The B species irreversible evolution to the A species form in the excited state produces the shorter component (τ_1 80–280 ps in Table 4) associated with the long decay component of the A conformer (τ_2 in Table 4). This leads to the more stable conformer A, with an interconversion rate constant k_{INT}, which is given by:

$$k_{INT} = \frac{1}{\tau_{short}} - \frac{1}{\tau_{long}} \cong \frac{1}{\tau_{short}}.$$

Values for k_{INT} are given in Table 4. The pre-exponential factors of the decays follow the relative abundances of each conformer. From Table 4 it can be seen that the interconversion rate constant, k_{INT}, is in the 10^9 s^{-1} to 10^{10} s^{-1} range.

As discussed above, the S_1 state dominant deactivation channel requires a structure with the two isatin-like half moieties perpendicular to

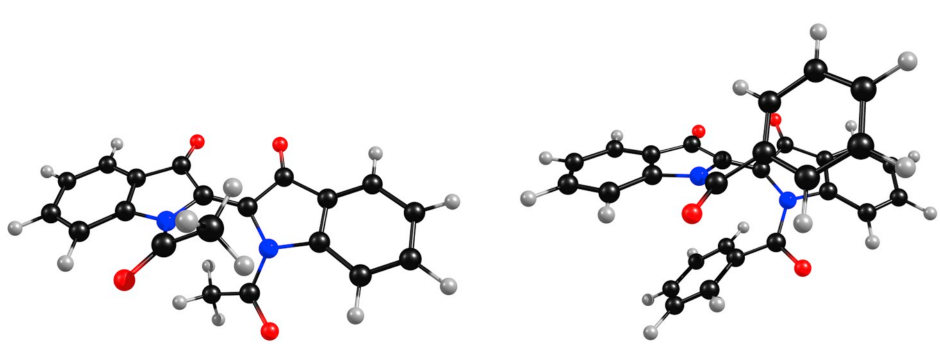

Fig. 7. The *cis* structures of **DAI** (left) and **DBI** (right) in a perspective that emphasizes the higher structural hindrance of **DBI**.

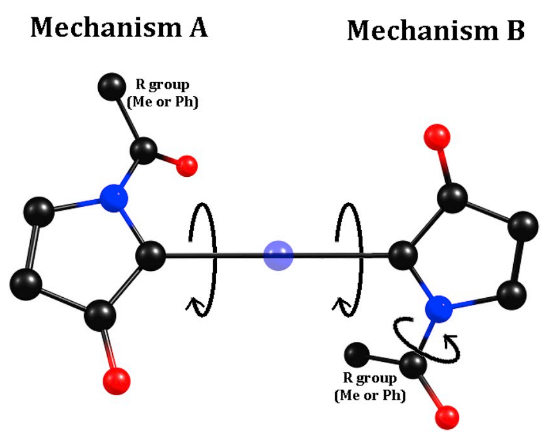

Fig. 8. Illustration of the two proposed mechanisms (A and B) of the dynamics for fluorescence bleaching from excitation geometries to CI.

each other and at least one C=O nearly planar with the isatin-like moiety, see Fig. 5.

Fig. 8 schematically illustrates two mechanisms (A and B) for the deactivation of S_1. With mechanism A, the A conformer (see Fig. 3) deactivation involves a single rotation around the central C–C bond on going from S_1 to S_0. In this mechanism no further rotation is observed, i.e., the carbonyl co-planarity with each one of the isatin-like moieties is already present. In the case of mechanism B in Fig. 8, besides the rotation around the C–C bond (present in mechanism A) an additional rotation of the acyl group (not present in mechanism A) is also occurring. Mechanism B in Fig. 8 corresponds to the deactivation of B conformers (for DAI and DBI in Fig. 3) from S_1 to S_0.

The requirement of carbonyl co-planarity with the isatin-like moiety can only be achieved (without acyl rotation) with the A conformer (mechanism A), whereas in the case of mechanism B (the only found possible for **DAI**) it corresponds to the longer component observed in the time resolved fluorescence measurements. The two mechanisms (A and B in Fig. 8) can be observed for **DBI,** where the longer component is associated with the deactivation of S_1 through mechanism B and the shorter to mechanism A. The associated pre-exponentials factors match the abundances of the corresponding isomers in Fig. 3 and Table 2.

Additional information on the excited-state deactivation processes in **DAI** and **DBI** was obtained from femtosecond (fs)-transient absorption (TA) measurements. Time-resolved transient absorption difference spectra (fs-TA) for these compounds in 2MeTHF were obtained with excitation at 530 nm and recorded in the 440–750 nm range for **DBI** within a time window of 227 ps and between 415 and 750 nm for **DAI** within a time window of 8 ns (Fig. 9).

From the fs-TA spectra of **DAI** and **DBI** no bleaching of the ground-state absorption was observed and positive TA bands at 415–500 nm, with maxima at ~430 nm for **DAI** (TDDFT predicts a $S_1 \rightarrow S_8$ band for the CI form at 466 nm) and ~460 nm for **DBI** ($S_1 \rightarrow S_8$ at 476 nm from TDDFT), together with absorptions at 550–650 nm (maxima ~598 nm for **DAI** and 611 nm for **DBI**, predicted by TDDFT to be an $S_1 \rightarrow S_7$ at 570 nm for **DAI** and $S_1 \rightarrow S_5$ at 626 nm for **DBI**) and 700–750 nm (maximum at ~730 nm for **DBI** but not detected in **DAI**) also corroborated by TDDFT which predicts a very weak $S_1 \rightarrow S_3$ band at 731 nm and 734 nm for **DAI** and **DBI** respectively. For a summary of these predicted and experimental transitions see Table SI1. These were attributed to the transient excited state absorptions of these two compounds at the CI geometry. Due to the orthogonality of the two half isatin-like moieties the singlet and triplet states should be nearly iso-energetic making it impossible to attribute the nature of the transients to excited state singlet or triplet absorption. Nevertheless it is worth reporting that for **DAI** the existence of a triplet state has been reported previously [26,42]

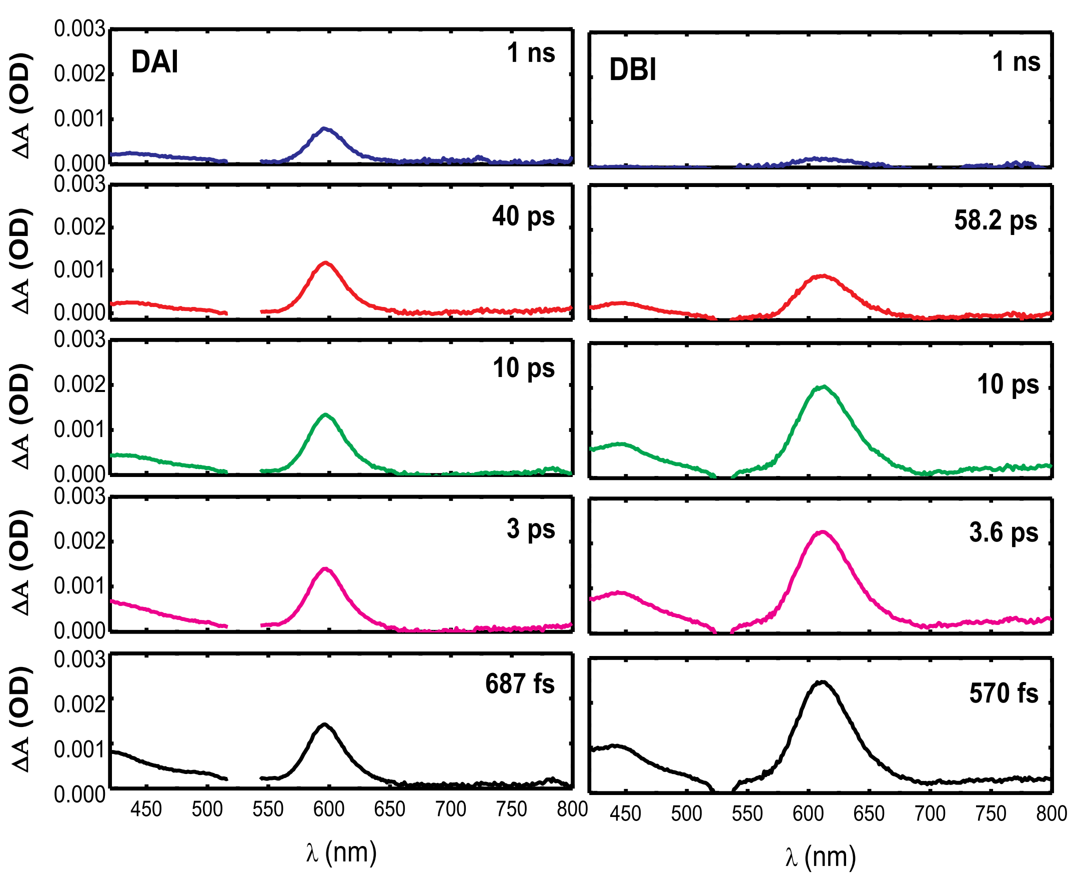

Fig. 9. fs-TA spectra for **DAI** (left) and **DBI** (right) obtained with pump @ 530 nm in 2MeTHF at T = 293 K.

and therefore cannot be completely ruled out as a competitive deactivation path of the excited state of this compound.

The data resulting from the fs-TA decays is given in Table 5. The decay times are very similar, but not identical, to those obtained from time resolved fluorescence data (Table 4). It is interesting to note that **DAI** presents two decay components, with the shorter component with a contribution (seen by the associated pre-exponential factor) smaller than the longer one. The absence of the shorter component in the fluorescence decays, and therefore the mono-exponential decay (Table 4) of DAI is due to the relative poor abundance of the associated conformer A (2% in Table 2) relative to conformer B (see Table 2). In the case of the fs-TA, the absorption of this conformer is observed.

With **DBI**, where the opposite is observed, the largest contribution comes from the fastest component. The relative contributions follow the relative abundances of the **A** and **B** conformers. The fact that the independent analysis at different wavelengths shows essentially identical amplitudes (a_i) and decay times (τ_i) in the fs-TA of **DBI** further supports the involvement of two conformers in the excited state behavior of this compound.

4. Conclusions

In this work, we present the spectral and photophysical properties of various indigo derivatives in which the hydrogen in the N–H groups has been replaced by acetyl (DAI, N,N′-diacethylindigo) and benzoyl (DBI, N,N′-dibenzoylindigo) groups. This precludes the excited state proton transfer in these compounds, thus allowing the observation of different deactivation routes (conformational changes) from the excited state. With **DAI**, rotation around the central carbon-carbon bond allows formation of the *cis* isomer, whereas with **DBI**, steric hindrance introduce geometric restrictions that leads to the presence of two conformers. This was confirmed by time-resolved fluorescence, fs-transient absorption and TDDFT calculations. In polar solvents the radiationless rate constants were found 2–3 orders of magnitude higher than the radiative rate constants, which were explained by a more accessible conical intersection of **DAI** and **DBI** derivatives.

Author contribution statement

Danîela C. Nobre performed the overall photophysical measurements including the different spectra (absorption and emission), the time-resolved fluorescence and fs-TA experiments with the support of Carla Cunha.

Alessandro Porciello, Federica Valentini, Assunta Marrocchi, and Luigi Vaccaro were responsible for the synthesis of the compounds. Luigi Vaccaro was also responsible by the design of the compounds and writing of the experimental procedures relative to the synthesis and analytical characterization of the compounds.

Adelino M. Galvão was responsible by the TDDFT calculations with the help of Danîela C. Nobre and J. Sérgio Seixas de Melo.

J. Sérgio Seixas de Melo was responsible by the idea, rationalization and writing of the manuscript.

Declaration of competing interest

The authors declare no conflict of interest.

Acknowledgements

This work was supported by project “Hylight”(n^{o}031625) 02/SAICT/2017 which is funded by Fundação para a Ciência e a Tecnologia (FCT), Portuguese Agency for Scientific Research, and COMPETE Centro 2020. We also acknowledge funding by FEDER (Fundo Europeu de Desenvolvimento Regional) through COMPETE (Programa Operacional Factores de Competitividade), Portugal. The Coimbra Chemistry Centre is supported by the FCT through the Project UID/QUI/00313/2019. CQE is also supported by FCT through the project UIDB/00100/2020 and UIDP/00100/2020. DCN acknowledges FCT for a PhD grant (SFRH/BD/140890/2018). F.V., A.P., A.M., L.V. gratefully acknowledge the Università degli Studi di Perugia and Ministero dell’ Istruzione, dell’Università e della Ricerca for financial support to the project AMIS, through the program “Dipartimenti di Eccellenza - 2018–2022”. The research leading to these results has received funding from Laserlab-Europe (grant agreement no. 284464, EC’s Seventh Framework Programme).

Appendix A. Supplementary data

Supplementary data to this article can be found online at https://doi.org/10.1016/j.dyepig.2020.108197.

References

[1] Melo MJ, Ferreira JL, Parola AJ, Seixas de Melo JS. Photochemistry for cultural heritage. In: Bergamini G, Silvi S, editors. Applied photochemistry: when light meets molecules. Cham: Springer International Publishing; 2016. p. 499–530.
[2] Seixas de Melo JS. The molecules of colour. Photochemistry, vol. 45. The Royal Society of Chemistry; 2018. p. 68–100.
[3] Seixas de Melo JS. The molecules of colour and Art. Molecules with history and modern applications. In: Albini A, Prodi S, editors. Photochemistry. London: RSC; 2020. p. 196–216.
[4] Klessinger M. The origin OF the color OF indigo dyes. Dyes Pigments 1982;3(2–3):235–41.
[5] Petermayer C, Dube H. Indigoid photoswitches: visible light responsive molecular tools. Acc Chem Res 2018;51(5):1153–63.
[6] Pina J, Sarmento D, Accoto M, Gentili PL, Vaccaro L, Galvão A, et al. Excited-state proton transfer in indigo. J Phys Chem B 2017;121(10):2308–18.
[7] Fang C, Durbeej B. Calculation of free-energy barriers with TD-DFT: a case study on excited-state proton transfer in indigo. J Phys Chem A 2019;123(40):8485–95.
[8] Nicholls-Allison EC, Nawn G, Patrick BO, Hicks RG. Protoisomerization of indigo di- and monoimines. Chem Commun 2015;51(62):12482–5.
[9] Mondal P, Chatterjee M, Paretzki A, Beyer K, Kaim W, Lahiri GK. Noninnocence of indigo: dehydroindigo anions as bridging electron-donor ligands in diruthenium complexes. Inorg Chem 2016;55(6):3105–16.
[10] Liu C, Dong S, Cai P, Liu P, Liu S, Chen J, et al. Donor–acceptor copolymers based on thermally cleavable indigo, isoindigo, and DPP units: synthesis, field effect transistors, and polymer solar cells. ACS Appl Mater Interfaces 2015;7(17):9038–51.
[11] Glowacki ED, Voss G, Demirak K, Havlicek M, Sunger N, Okur AC, et al. A facile protection-deprotection route for obtaining indigo pigments as thin films and their applications in organic bulk heterojunctions. Chem Commun (J Chem Soc Sect D) 2013;49(54):6063–5.
[12] Głowacki ED, Voss G, Sariciftci NS. 25th anniversary article: progress in Chemistry and applications of functional indigos for organic electronics. Adv Mater 2013;25(47):6783–800.
[13] Farka D, Scharber M, Głowacki ED, Sariciftci NS. Reversible photochemical isomerization of N,N′-Di(t-butoxycarbonyl)indigos. J Phys Chem A 2015;119(15):3563–8.
[14] Dittmann M, Graupner FF, Maerz B, Oesterling S, deVivie-Riedle R, Zinth W, et al. Photostability of 4,4′-dihydroxythioindigo, a mimetic of indigo. Angew Chem Int Ed Engl 2014;53(2):591–4.
[15] Boice G, Patrick BO, McDonald R, Bohne C, Hicks R. Synthesis and photophysics of thioindigo diimines and related compounds. J Org Chem 2014;79(19):9196–205.
[16] Rondão R, Seixas de Melo JS. Thio-Mayan-like compounds: excited state characterization of indigo sulfur derivatives in solution and incorporated in palygorskite and sepiolite clays. J Phys Chem C 2013;117(1):603–14.
[17] Pereira RC, Pineiro M, Galvão AM, Seixas de Melo JS. Thioindigo, and sulfonated thioindigo derivatives as solvent polarity dependent fluorescent on-off systems. Dyes Pigments 2018;158:259–66.
[18] Volkov VV, Chelli R, Righini R, Perry CC. Indigo chromophores and pigments: structure and dynamics. Dyes Pigments 2020;172:107761.
[19] Moreno M, Ortiz-Sanchez JM, Gelabert R, Lluch JM. A theoretical study of the photochemistry of indigo in its neutral and dianionic (leucoindigo) forms. Phys Chem Chem Phys 2013;15(46):20236–46.
[20] Yamazaki S, Sobolewski AL, Domcke W. Molecular mechanisms of the photostability of indigo. Phys Chem Chem Phys 2011;13(4):1618–28.
[21] Nakagawa H, Matsumoto A, Daicho A, Ozaki Y, Ota C, Nagasawa Y. Solvent dependent trans→cis photoisomerization of N, N′-diacetylindigo studied by femtosecond time-resolved transient absorption spectroscopy. J Photochem Photobiol A Chem 2018;358:308–14.
[22] Huang C-Y, Bonasera A, Hristov L, Garmshausen Y, Schmidt BM, Jacquemin D, et al. N′-Disubstituted indigos as readily available red-light photoswitches with tunable thermal half-lives. J Am Chem Soc 2017;139(42):15205–11.
[23] Huber Ludwig A, Mayer P, Dube H. Photoisomerization of mono-arylated indigo and water-induced acceleration of thermal cis-to-trans isomerization. ChemPhotoChem 2018;2(6):458–64.

[24] Giuliano CR, Hess LD, Margerum JD. Cis-trans isomerization and pulsed laser studies of substituted indigo dyes. J Am Chem Soc 1968;90(3):587–94.
[25] Pouliquen J, Wintgens V, Toscano V, Jaafar BB, Tripathi S, Kossanyi J, et al. Photoisomerization of N,N′-disubstituted indigos. A search for energy storage. Can J Chem 1984;62(11):2478–86.
[26] Gorner H, Pouliquen J, Kossanyi J. Trans to cis photoisomerization of N,N'-Disubstituted indigo dyes via excited singlet-states - a laser flash-photolysis and steady-state irradiation study. Can J Chem 1987;65(4):708–17.
[27] Seixas de Melo J, Moura AP, Melo MJ. Photophysical and spectroscopic studies of indigo derivatives in their keto and leuco forms. J Phys Chem A 2004;108: 6975–81.
[28] Pina J, Seixas de Melo J, Burrows HD, Maçanita AL, Galbrecht F, Bunnagel T, et al. Alternating binaphthyl-thiophene copolymers: synthesis, spectroscopy, and photophysics and their relevance to the question of energy migration versus conformational relaxation. Macromolecules 2009;42(5):1710–9.
[29] Striker G, Subramaniam V, Seidel CAM, Volkmer A. Photochromicity and fluorescence lifetimes of green fluorescent protein. J Phys Chem B 1999;103(40): 8612–7.
[30] Pina J, Seixas de Melo JS, Eckert A, Scherf U. Unusual photophysical properties of conjugated, alternating indigo-fluorene copolymers. J Mat Chem 2015;3(12): 6373–82.
[31] Schmidt MB KK, Boatz JA, Elbert ST, Gordon MS, Jensen JH, Koseki S, Marsunaga N, Nguyen KA, Su S, Windus TL, Dupuis M, Mongomery Jr JA. General atomic and molecular electronic structure system. J Comput Chem 1993;14(11): 1347–63.
[32] Yanai T, Tew DP, Handy NC. A new hybrid exchange–correlation functional using the Coulomb-attenuating method (CAM-B3LYP). Chem Phys Lett 2004;393(1–3): 51–7.
[33] Jacquemin D, Perpete EA, Scuseria GE, Ciofini I, Adamo C. TD-DFT performance for the visible absorption spectra of organic dyes: conventional versus long-range hybrids. J Chem Theory Comput 2008;4(1):123–35.
[34] Lüttke W, Hermann H, Klessinger M. Theoretically and experimentally determined properties of fundamental indigo chromophore. Angew Chem Int Ed Engl 1966;5 (6):598–9.
[35] Seixas de Melo JS, Rondão R, Burrows HD, Melo MJ, Navaratnam S, Edge R, et al. Spectral and photophysical studies of substituted indigo derivatives in their keto forms. ChemPhysChem 2006;7:2303–11.
[36] Seixas de Melo J, Rondão R, Burrows HD, Melo MJ, Navaratnam S, Edge R, et al. Photophysics of an indigo derivative (keto and leuco structures) with singular properties. J Phys Chem A 2006;110:13653–61.
[37] Weinstein J, Wyman GM. Spectroscopic studies on dyes. II. The structure of N,N'-Dimethylindigo. J Am Chem Soc 1956;78(16):4007–10.
[38] Wyman GM, Zenhause AF. Spectroscopic studies on dyes .V. Derivatives of cis-indigo. J Org Chem 1965;30(7):2348–52.
[39] Bartocci G, Spalletti A, Mazzucato U. Conformational aspects of organic photochemistry. In: Waluk J, editor. Conformational analysis of molecules in excited states. first ed. New York: Wiley-VCH; 2000. p. 237–96.
[40] Flom SR, Nagarajan V, Barbara PF. Dynamic solvent effects on large-amplitude isomerization rates. 1. 2-Vinylanthracene. J Phys Chem 1986;90(10):2085–92.
[41] Rondão R, Seixas de Melo J, Melo MJ, Parola AJ. Excited-state isomerization of leuco indigo. J Phys Chem A 2012;116(11):2826–32.
[42] Görner H, Schulte-Frohlinde D. Laser flash studies of thioindigo and indigo dyes. Evidence for a trans configuration of the triplet state. Chem Phys Lett 1979;66(2): 363–9.